Experimental Validation of Planck's Constant through Electron Diffraction

I. Singh

Department of Physics, Purdue University, West Lafayette, Indiana 47907

PHYS 340

20 November 2023

Abstract

Wave-particle duality, or the seemingly paradoxical way quanta act as both waves and particles, has long been of interest to physicists. Significant historical experiment has been dedicated to its research, most prominently including de Broglie's landmark paper that proposed a model for the wave-particle duality of particles beyond light, namely electrons. This experiment aimed to validate that model by using frameworks of electron diffraction off a Gold lattice to measure diffraction ring radii and estimate Planck's constant. Through the slope of a LSRL that incorporated de Broglie's theoretical developments, Planck's constant was estimated to be $6.419 * 10^{-34}$ Js with a correlation coefficient of 0.9985. That value differs from the accepted value of $6.626 * 10^{-34}$ Js by 3.124%, and quantitatively validates the wave-particle duality for the electron. This experiment prompts further investigation into whether matter is inherently wave-particle dual at scales even larger than the electron.

Introduction and Theory

The wave-particle nature of light has long been of interest to modern physicists. Contradicting evidence that shows light's observability of quantized particles that undergo wave-like phenomena led to differing views about its true nature that date as far back as the dawn of the 18th century (Huygens, 1690; Newton, 1704). The rich experimental history built upon those landmark historical viewpoints most prominently includes Young's double slit experiment, which famously observed significant interference patterns through a double slit setup that delocalized diffracted light (Young, 1804). That experiment proved beyond a doubt that light displays the strange property that is now called *wave-particle duality*.

In 1923, Louis de Broglie published his landmark paper that argued that all particles at a small enough scale display the wave-particle duality well documented in light (de Broglie, 1923). This experiment aims to experimentally confirm the theoretical basis of de Broglie's argument by quantitatively analyzing diffraction, an inherently wave-like process, in electrons, whose quantization is well established. In doing so, the groundwork for quantum mechanics will be experimentally shown via implicit demonstration of the fact that all matter could display wave-particle duality.

In his paper, de Broglie posits that the wavelength of an electron is given by Planck's constant divided by the electron's momentum (de Broglie, 1923). Combining that information with the kinetic energy of an electron, the below derivation leads to equation 1 as for the electron wavelength λ.

$$\lambda = \frac{h}{p} = \frac{h}{mv}.$$

$$KE = eV = \frac{mv^2}{2}.$$

$$\frac{2eV}{v} = mv \rightarrow v = \sqrt{\frac{2eV}{m}} \rightarrow \lambda = \frac{h}{m\sqrt{\frac{2eV}{m}}}.$$

$$\lambda = \frac{h}{\sqrt{2meV}}. \quad \text{(Equation 1)}$$

In that equation, h is Planck's constant ($6.626 * 10^{-34}$ m^2kg/s), m is the electron mass ($9.109 * 10^{-31}$ kg), e is the electron charge ($1.602 * 10^{-19}$ C), and V is the voltage potential applied on the electron in Volts (Tiesinga et al, 2018).

To quantitatively verify that equation, which would in turn verify de Broglie's theoretical claims, another model of electron diffraction in a crystal must be developed. In crystals, atoms form a series of parallel planes in directions that can be described as ordered pairs of (h, k, l), where each letter is known as a *Miller index* (note that h here is unrelated to Planck's constant). Since a gold lattice, which has a face-centered cubic crystal, will be used in this experiment, only the Miller planes possible for a face-centered cubic crystal are relevant here. The triplet pairs for those planes are given in figure 1 below.

Figure 1: Relevant Miller triplets for Gold

h k l
111
200
220
311
222
400
331

If the beam diffracts from the incident direction by an angle θ, then the derivation shown below can be used to arrive at equation 2 as an expression of wavelength based on (H, K, L).

$$n\lambda = 2d\sin\theta, \sin\theta \approx \theta = \frac{r}{2D}, d = \frac{a}{\sqrt{h^2+k^2+l^2}}.$$

$$\lambda = \frac{2a\sin\theta}{n\sqrt{h^2+k^2+l^2}} = \frac{2a\sin\theta}{\sqrt{H^2+K^2+L^2}} = \frac{ar}{D\sqrt{H^2+K^2+L^2}}.$$

$$\lambda = \frac{a}{D} * \frac{r}{\sqrt{H^2+K^2+L^2}} \text{ (Equation 2)}.$$

The 3 equations given in the first line are the Bragg's condition for diffraction, a trigonometric relationship for ring diffraction radius, and a fundamental relationship from the Miller indices. The parameters of equation 2 given at the end of the derivation are the radius of diffraction r, the gold lattice constant a ($4.0786 * 10^{-10}$ m), the distance between the diffracting crystal plane and the particle reception plane D ($2.56 * 10^{-1}$ m), and a constant from the n^{th} order diffraction of (h, k, l) represented as the first order diffraction of (H, K, L) as $(H^2+K^2+L^2)^{½}$ (PHYS 340 LAB MANUAL). Equation 2 will be used to convert all radius measurements into wavelength values so that equation 1 can be directly used in data analysis.

Methods

The electron diffraction apparatus is a Lambda Scientific LEAI-62, whose bird's eye view is diagrammed in figure 2 below.

Figure 2: Bird's Eye View of Experimental Apparatus

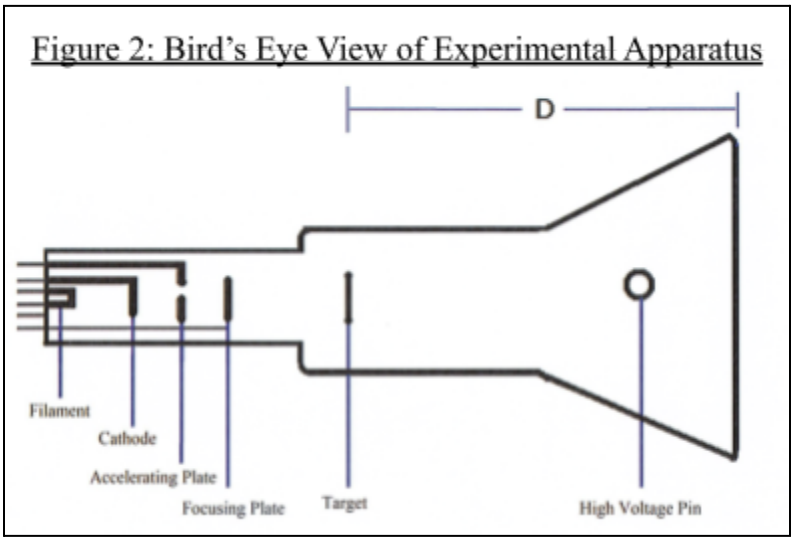

The filament heats the cathode to thermionically emit electrons that are then accelerated through a controllable voltage at 0.1 kV resolution, focused onto the target crystal, and deflected onto the final surface at the far right of the figure.

Beginning with the voltage set to 12 kV, the LEAI-62 was given about 1 minute to settle into a stable position after calibration of the ring center to the center of the screen surface. An image was then taken of the rings with a millimeter accuracy ruler over their diameter, and radius measurements were taken by determining the locations of highest ring intensity in ImageJ. This process was repeated at 14, 16, 18, and 20 kV, leading to a total of 5 images that gave 7 radius measurements each.

As stated, radii were measured using ImageJ for maximum precision, with the maximum intensity for each ring being recorded as that ring's voltage. Since ImageJ was used only for objective determination of the location of maximum intensity in each ring, the precision was still limited by the ruler itself; as such, measurements were taken only at 0.5 mm levels. For each image, radius measurements were matched to HKL triplets based on the relationship between radius and $(H^2 + K^2 + L^2)^{1/2}$ predicted by equation 2 (see figure 3 below), which provided the complete raw data.

Figure 3: Labeled rings from an example set of rings (not used in data)

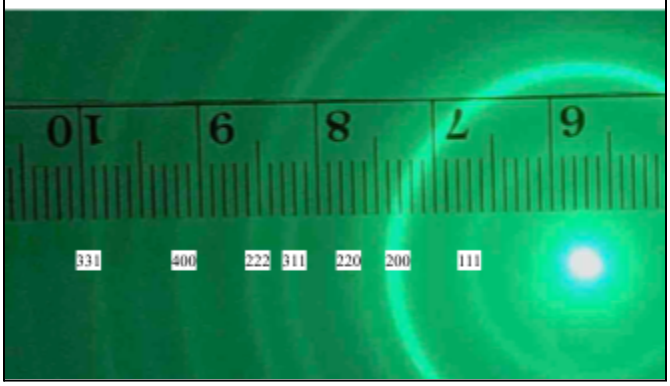

Results

In data collection, due to an unknown issue in the LEAI-62, rings appeared to be slightly elliptical. As such, diffraction radii of the ellipses were approximated as the average of the

longest radius (semi-major axis) and its orthogonal counterpart (semi-minor axis). They are shown in millimeters in figure 4 below for each Miller triplet. From the raw radii data, it is clear that accelerating voltage accompanies a decreasing radius, which in conjunction with equation 2's prediction that radius and wavelength are directly associated, gives a preliminary verification of the inverse relationship equation 1 predicts between voltage and wavelength.

Figure 4: Observed Diffraction radii in millimeters at varying voltages for each Miller triplet

HKL	12 kV r (mm)	14 kV r (mm)	16 kV r (mm)	18 kV r (mm)	20 kV r (mm)
111	9.5	10	9.5	9	8
200	11.5	11	11	9	9
220	18.5	16.5	15.5	15.5	13.5
311	21	19	18	17	17
222	27.5	25.5	24.5	21.5	21
400	32	27.5	26	25	23
331	37.5	32.5	28.5	27.5	25

This data was converted into values compatible with LSRL analysis of equation 1 (see appendix A). The composite LSRL is plotted in figure 5 below.

Figure 5: Composite Plot of 1/V by Wavelength Squared for an Estimate of Planck's Constant via LSRL Slope

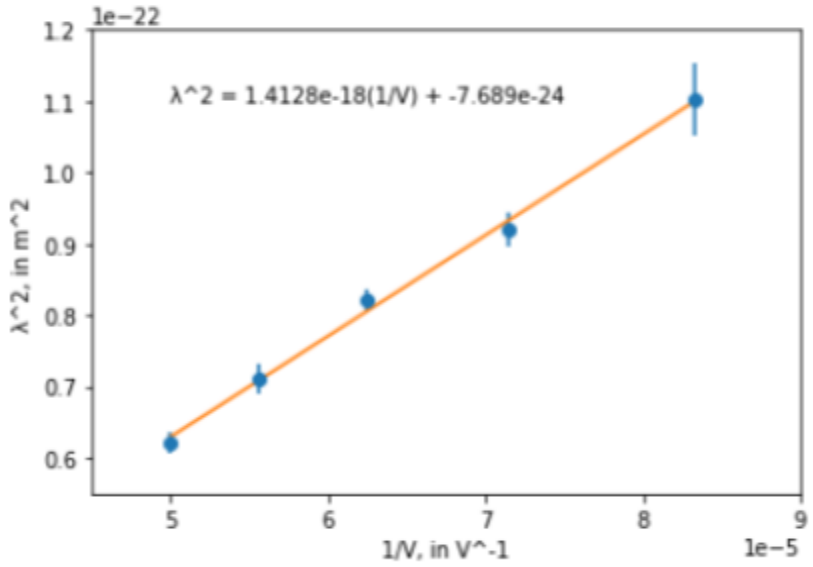

The model slope taken in conjunction with electron mass m ($9.109 * 10^{-31}$ kg) and electron charge ($1.602 * 10^{-19}$ C) yields an estimate of $6.419 * 10^{-34}$ Js for Planck's constant h (see appendix A). This differs from the accepted value of $6.626 * 10^{-34}$ Js by 3.124%. The low 3.124% error in the aforementioned estimate of Planck's constant quantitatively validates the models used for the regression, thus verifying de Broglie's original formulation that electron wavelength is Planck's constant divided by momentum. By extension, this verifies the diffraction model developed in equation 2, and confirms the wave-particle duality of light discussed in the introduction.

Discussion

This experiment successfully demonstrated the wave aspect of light via quantitative analysis of electron diffraction through a gold lattice. Since the observations of the inherently wave-like phenomenon of diffraction in this experiment validated models that incorporated particle-like properties of electrons (namely mass), the low percent error of 3.124% also extends this experiment's results to imply the wave-particle duality of electrons. The relative error sizes for voltages and radii shown in figure A2 (see appendix A) are quite small, so although the correlation coefficient of 0.9985 for the LSRL does not incorporate the size of those errors, it is reasonable to assume that the propagation of error from measurement uncertainties is insignificant in the estimate of Planck's constant. That being said, it should be acknowledged that the correlation coefficient's value is inflated by taking each voltage's distribution of 7 data points as a single average.

This experiment supports de Broglie's proposition that all matter inherently displays wave-particle duality by proving that the paradoxical phenomenon is observable in non-photon particles. Further research is necessary to determine if the conclusions of this experiment are

generalizable to all matter, but it is not a stretch of the imagination to hypothesize that at a scale similar to electrons, all matter does indeed display wave-particle duality.

Of course, 3.124% error is not perfect, and there were problems in data collection that may have systematically skewed the results. Most prominently, it was mentioned that the diffraction rings were observed to be elliptical rather than perfectly circular. Although the adjustment of averaging the semi-major and semi-minor axes to get a "radius" was made, that assumes that the diffraction circles were skewed by the same amounts in the major and minor directions, which may not be a valid assumption. It was impossible to fix the apparatus due to the time constraint, but future experiments should take care to either ensure circular diffraction rings or perform more comprehensive analysis on the semi-minor and semi-major axes separately.

Furthermore, although the use of ImageJ improved precision in radius measurement, ultimately the uncertainty of the plastic ruler placed on the diffraction screen led to irreducible error due to the ruler's inherent uncertainty. Taking averages to obtain the "circular" radius measurement exacerbated the ruler's uncertainty by adding another step of error propagation. Further investigations on diffraction rings could investigate ways of precisely measuring radii directly on the screen with the rings itself, rather than using an extra ruler, to minimize uncertainty.

A better estimate of Planck's constant could have been derived if more data points were taken, either by repeating the cycle of voltages multiple times for multiple trials, or by including more voltages less far apart and above 20 kV or below 12 kV. That being said, a 3.124% error in estimation of Planck's constant is good by most standards, so any improvements to the data collection process of this experiment may be rendered useless simply due to limitations of the LEAI-62.

Conclusion

This electron diffraction experiment determined Planck's constant to be $6.419 * 10^{-34}$ Js, a value that differed from the accepted value of $6.626 * 10^{-34}$ Js by 3.124% error. Despite some systemic issues in data collection, the experiment overall successfully demonstrated the wave-particle duality of electrons by using models that incorporated particle-like frameworks to analyze wave-like diffraction data. This proof of the wave-particle duality of electrons is the first step towards a possible wave-particle duality inherent to all matter, for which significant future experimental efforts should be devoted.

Acknowledgement

I would like to thank the TAs and professor of PHYS 340 from the Physics Department of Purdue University for their help in performing the labs, troubleshooting small issues with the apparatus, and the supply of lab manuals they gave.

References

de Broglie, L. (1923). Waves and Quanta. *Nature,* 112(2815), 540. https://doi.org/10.1038/112540a0

Huygens, C. (1690). *Traité de la lumière où sont expliquées les causes de ce qui luy arrive dans la reflexion, & dans la refraction, et particulierement dans l'etrange refraction du cistal d'Islande.* Pierre van der Aa.

LEAI-62 Electron Diffraction Apparatus. (n.d.). Lambda Scientific Systems, Inc.

Newton, S. I. (1704). *Opticks: Or, A Treatise of the Reflexions, Refractions, Inflexions and Colours of Light.* S. Smith, and B. Walford.

PHYS 340 LAB MANUAL

Tiesinga, E., Mohr, P.J., Newell, D. B., & Taylor, B. N. (2019). *The 2018 CODATA Recommended Values of the Fundamental Physical Constants* (Web Version 8.1). National Institute of Standards and Technology, Gaithersburg, MD 20899.

Young, T. (1804). *The Bakerian Lecture. Experiments and calculations relative to physical optics*. Retrieved from https://royalsocietypublishing.org/doi/10.1098/rstl.1804.0001.

Appendix A

To convert radius measurements into wavelengths, a linear equation was used. Figure A1 shows this process, with the final wavelengths for each Miller triplet reported in figure A1(iii).

Figure A1: Conversion of Radii Measurements into Wavelengths

HKL indices	HKL Constant	a/(D * HKL) = Q
111 HKL	1.73E+00	9.20E-10
200 HKL	2.00E+00	7.97E-10
220 HKL	2.83E+00	5.63E-10
311 HKL	3.32E+00	4.80E-10
222 HKL	4.00E+00	3.98E-10
400 HKL	4.36E+00	3.66E-10
331 HKL	4.90E+00	3.25E-10

$$Q = \frac{a}{D\sqrt{H^2 + K^2 + L^2}}$$

$$\lambda = Q * r$$

Q	12 kV λ (nm)	14 kV λ	16 kV λ	18 kV λ	20 kV λ
9.20E-10	8.74E-03	9.20E-03	8.74E-03	8.28E-03	7.36E-03
7.97E-10	9.16E-03	8.76E-03	8.76E-03	7.17E-03	7.17E-03
5.63E-10	1.04E-02	9.30E-03	8.73E-03	8.73E-03	7.61E-03
4.80E-10	1.01E-02	9.13E-03	8.65E-03	8.17E-03	8.17E-03
3.98E-10	1.10E-02	1.02E-02	9.76E-03	8.56E-03	8.36E-03
3.66E-10	1.17E-02	1.01E-02	9.51E-03	9.14E-03	8.41E-03
3.25E-10	1.22E-02	1.06E-02	9.27E-03	8.94E-03	8.13E-03

Figure A1(i) (top left): Miller triplets written as HKL, the value of $(H^2 + K^2 + L^2)^{½}$ as the HKL constant, and the composite Q constant calculated via substitution into the top equation shown in figure 5b
Figure A1(ii) (top right): Equation to calculate Q from a, D, and $(H^2+K^2+L^2)$
Figure A1(iii) (bottom): Wavelengths corresponding to radii from figure 4 calculated via the bottom equation in figure 5b

To perform regression analysis using equation 1, data for each voltage were averaged to a single predicted wavelength value. These averages, along with errors corresponding to the voltages and wavelengths, are reported in figure A2 below. Absolute uncertainty in voltage was constant due to the LEAI-62's voltage reporting precision; absolute uncertainty in wavelength for each voltage was taken as the standard deviation of the wavelength distributions for each voltage.

Figure A2: Voltage and averaged wavelength values with corresponding absolute and relative uncertainties

V (kV)	Abs Unc in V (kV)	Rel Error in V	Observed Avg λ (nm)	Abs Unc in Avg λ (nm)	Rel Error in Avg λ
12	5.00E-02	4.17E-03	1.05E-02	4.77E-04	4.56E-02
14	5.00E-02	3.57E-03	9.59E-03	2.50E-04	2.61E-02
16	5.00E-02	3.13E-03	9.06E-03	1.69E-04	1.86E-02
18	5.00E-02	2.78E-03	8.43E-03	2.47E-04	2.93E-02
20	5.00E-02	2.50E-03	7.89E-03	1.90E-04	2.40E-02

To perform regression, the reciprocal of voltage was plotted by wavelength squared. The process of developing and plotting those composite data points is shown in figure A3. Figure A3(iii) was shown in the text; the slope of the fitted LSRL is $m = 1.412 * 10^{-18}$, the y-intercept $b = -7.689 * 10^{-24}$, and the correlation coefficient $r = 0.9985$. Further analysis of these values is given in the text.

Figure A3: Composite Averages for Regression Analysis and Estimation of Planck's Constant

1/V (V^-1, E5)	Abs Error in 1/V (V^-1)	λ^2 (m^2, E22)	Abs Error in λ^2 (m^2, E22)
8.333333333	3.47E-02	1.09520157	5.00E-02
7.142857143	2.55E-02	0.9205815199	2.40E-02
6.25	1.95E-02	0.8206251126	1.53E-02
5.555555556	1.54E-02	0.7102307276	2.08E-02
5	1.25E-02	0.6219093751	1.50E-02

$$\lambda^2 = \frac{h^2}{2me} * \frac{1}{V}$$

$$m = \frac{h^2}{2me} = 1.412 * 10^{-18}$$

$$b = -7.689 * 10^{-24}$$

$$r = +0.9985$$

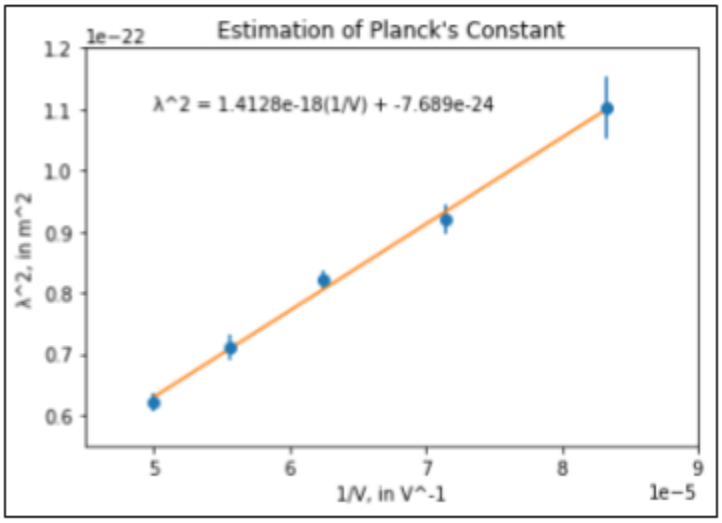

Figure A3(i) (top): Composite data for regression analysis with absolute errors graphed as error bars; errors in 1/V were too small to display
Figure A3(ii) (bottom left): Regression model and LSRL parameters
Figure A3(iii) (bottom right): Plot between wavelength squared and reciprocal voltage plot for estimation of Planck's constant. X scaled by 10^{-5}, Y scaled by 10^{-22} for wavelength squared.